Journal of Chromatography, 265 (1983) 1–18
Elsevier Science Publishers B.V., Amsterdam — Printed in The Netherlands

CHROM. 15,880

USE OF LIGHT SCATTERING AS A DETECTOR PRINCIPLE IN LIQUID CHROMATOGRAPHY

ANDRZEJ STOLYHWO*, HENRI COLIN and GEORGES GUIOCHON*
Laboratoire de Chimie Analytique Physique, École Polytechnique, 91128 Palaiseau (France)
(Received March 25th, 1983)

SUMMARY

The detector described is based on the large difference between the vapour pressure of solvents commonly used in liquid chromatography and that of most analytes, which thus permits phase separation between them. The column eluate is nebulized in a stream of warm gas in which the solvent vaporizes. Downstream, the particles of non-volatile analytes scatter the light of a laser beam. Part of the scattered light is collected and fed to a photomultiplier and the resulting signal is recorded. The detector responds to the mass flow of solutes, which makes it especially suitable for use with narrow-bore columns. The contribution of the detector to band broadening is between 0.1 and 0.2 μl. The baseline is very stable even with a steep concentration gradient, as illustrated by the analysis of triglycerides. The response is not linear but proportional to the power 1.8 of the mass flow of analyte. The detection limit is around 150 ng/sec for non-volatile compounds which are liquid at detector temperature. Possible improvements are discussed.

INTRODUCTION

Liquid chromatography is mainly carried out using light absorption detectors such as UV photometers and spectrophotometers (UVD) and, to a lesser extent, refractive index detectors (RID). These detectors constitute the main workhorses in the field[1].

The sensitive detection of compounds having weak absorption bands in the range of 200–400 nm such as sugars and fats is, however, very difficult with absorption detectors. The use of the more universal RID is also restricted in practice because of its poor detection limit and its high sensitivity to small fluctuations of chromatographic experimental conditions, such as flow-rate, solvent composition and temperature[2]. Moreover, if the separation of complex samples requires the use of gradient elution, the application of RID becomes almost impossible. Although for some solutes the use of either a reaction detector (RD) or a fluorescence detector (FD) is possible, this is not a general solution. In that respect, the LC analysis of complex

* On leave from the Institute of Organic Chemistry and Food Technology, Technical University Politechnika Gdanska, Gdansk, Poland.

0021-9673/83/$03.00

natural mixtures of lipids or sugars remains difficult owing to the lack of a suitable detector.

The problem becomes even worse when the use of narrow-bore columns is contemplated for the sake of solvent economy or better sensitivity because the sample size available is limited[3].

The miniaturization of detector cells is also extremely difficult and the technological problems have not yet been solved, because the detection limit should also be decreased or, at least, kept constant[2–6]. Some progress in the design of very small cells for UVD and FD has been reported[3–7], but the miniaturization of RD and RID seems much more difficult in spite of some interesting suggestions[8]. Similarly, the development of open-tubular columns is plagued by the lack of a suitable detector with a small contribution to band broadening, *i.e.*, an effective cell volume of the order of 1 nl[4,5]. Some interesting suggestions have been made for the use of new detector principles[8,9], but the information is scanty.

A non-selective detector more sensitive than the RID and easier to use, with a small contribution to band broadening, is thus seriously needed. The mass spectrometer would be a good solution if it were not so complex[10] and expensive. The electron-capture detector (ECD)[11] and flame-based detectors have been suggested[12]. Both are very sensitive and could be made with very small volumes. The ECD can be used only with volatile analytes, unfortunately, and it is very selective. Both ECD and flame-based detectors are very sensitive to the solvent flow-rate, and noisy signals are often encountered. The adaptability of these detectors to packed columns is thus difficult. This explains probably why the ECD has been practically abandoned.

The evaporative analyser[13,14] is an alternative solution which seems very attractive for a number of reasons. As most analytes in LC have a very low vapour pressure at room temperature, whereas the solvents used as the mobile phase have a large or at least significant vapour pressure, some kind of phase separation is conceivable. In fact, this is the basis for the transport detector[15–19] of which the detector discussed here is a modified version with no mechanical conveyor, thus eliminating the source of much complexity and trouble.

The aim of this paper is to describe a detector incorporating many features of advanced instrumentation, to discuss its performance and to demonstrate several advantages that are of major importance in connection with its application to narrow-bore packed columns.

THEORY

The principle of this detector is to nebulize the column effluent into a stream of tiny droplets carried down a short drift tube by a driving gas; the solvent is vaporized and the remaining droplets then cross a narrow light beam. Light scattered by the residual droplets made of material non-volatile under the conditions of experiment is collected and is a measure of the concentration of the solute in the column effluent. The temperature of the gas stream and its flow-rate should be sufficiently large to ensure total vaporization of the solvent before the droplets cross the light beam. The diameter of the drift tube should be large enough to allow the time necessary for the solvent vaporization without creating excessive delay in the transport. Background signal and noise would then originate mainly from solvent impurities including fine

silica particles[20]. This noise can be reduced by using tight filters or frits in the gas and solvent lines, and solvents with a very small content of non-volatile impurities.

Current Venturi-type nebulizers give droplets in the 2–20 μm range. Alternatively, the use of a diaphragm with a 2–10 μm diameter pinhole would provide a jet of droplets about twice as large as the pinhole, with a narrow size distribution[21], but at the cost of a pressure drop which is around 1 atm/μl · min of flow-rate for a 2-μm hole[21]. The pressure drop decreases in proportion to the fourth power of the inverse of the hole diameter. A typical efficient 1 mm I.D. column packed with 3–5-μm particles has an optimal flow-rate of 60–100 μl/min. Under these conditions, the additional pressure drop created by 5-μm or larger holes may be neglected.

The droplets shrink during vaporization of the solvent. Assuming that the concentration of non-volatile impurities in the mobile phase is 1 ppm (a reasonable if somewhat demanding specification) the size of the droplets of solvent impurities after total solvent vaporization will be 100 times smaller than that of the original droplets, *i.e.*, between 200 and 2000 Å with a nebulizer and around 1000 Å with a 5-μm hole diaphragm. This constitutes the background signal. Lower backgrounds require very thorough solvent purification.

The largest concentrations observed in analytical LC at the column outlet are of the order of 1 % (w/w); the reduction in size of the droplets made with such solutions is only a factor 4.6, so the droplets given by a conventional nebulizer are then roughly 0.4–4.5 μm in diameter while those given by a diaphragm are approximately 1–2 μm in diameter.

It is important to realize that, for a given set of experimental conditions, the elution of a peak will not be accompanied by a change in the number of droplets carried out through the system, but merely by a change in their diameters. As the intensity of scattered light is a very steep function of particle diameter, this size change provides the signal. Unfortunately, the relationship between particle size and intensity of scattered light is very complex when the ratio of the wavelength to the particle diameter is between 0.1 and 10. Although the use of an electromagnetic radiation beam with a wavelength longer than 50–100 μm or shorter than 20–40 Å would ensure a well defined relationship at any scattering angle, such a beam is very difficult to generate. The response of the detector could, in principle, be extracted from Mie's theory[22], but this derivation is outside the scope of this work.

We know, however, that the intensity of scattered light is a function of the complex refractive index of the material, *i.e.*, its refractive index and absorption coefficient. Thus, the response factor may vary from compound to compound. The intensity of light of a given wavelength, λ, scattered in a given direction by a droplet of diameter d, depends on the angle θ between this direction and that of the incident light beam and the ratio d/λ. A polar plot of the intensity of scattered light as a function of θ has the shape of a daisy. The size of the petals and their number change markedly with d/λ, so the amount of light scattered in a given direction by a stream of identical droplets does not increase regularly with increasing diameter.

The amount of light collected corresponds to the integration over a significant fraction of the space of the light scattered by each droplet. Further, the size distribution of droplets is relatively wide, so there is no preferred direction for collection of scattered light, and the signal increases monotonously with the average size of the droplet. The solid angle within which collection of scattered light should be made for maximal signal-to-noise ratio has to be determined experimentally.

EXPERIMENTAL

Fig. 1 shows a block diagram of the system. Carbon dioxide is selected as the driving gas because of its large specific heat, its ready availability and its low cost. Chemical purity is not important as long as there is no fine dust or oil mist from compressors. Two Millipore filters are used. The gas stream is delivered through a Brooks 86018 pressure controller (Brooks Instrument Division, Hatfield, PA, U.S.A.) and a Brooks 8902 flow-rate controller. A flow meter and an oven complete this gas line, which is thermally insulated from 6 to 8 in Fig. 1. The oven (6) is a coiled tube 50 cm × 0.5 mm I.D. enclosed in a temperature-controlled copper block. Typically, the oven temperature is set at 30°C and the temperature of the drift tube at approximately 40–50°C with all solvents that do not contain water. The detector consists of a nebulizer, a diffusion or drift tube enclosed in a heated copper block and a light-scattering cell. The exhaust from the detector is directed to a water aspirator operated slightly below atmospheric pressure. It is very important to realize that this detector turns the whole column effluent into a gas stream containing toxic solvent vapours and possibly more toxic sample particles. This stream should be vented in a way that avoids intoxication of laboratory personnel and harm to the environment.

A Hughes 3225H-Pc 1-mW helium–neon laser (Hughes Aircraft Company, Carlsbad, CA, U.S.A.) delivers a red light beam at 632 nm across the light cell to a light trap. The scattered laser light is collected by a glass rod and transmitted through a short optical fibre to an RCA type R-372 photomultiplier (Hamamatsu, Middlesex, NJ, U.S.A.) which is polarized by a Keithley type 240A high-voltage supply (Keithley Instruments, Cleveland, OH, U.S.A.). The photomultiplier current is amplified using a Keithley type 417K electrometer and recorded on a Servotrace recorder (Sefram, Paris, France).

The use of a flexible optical fibre to connect the light-scattering cell to the photomultiplier simplifies the mechanical construction of the detector. This also permits the transmission of low-level signals as this light conductor is insensitive to all sources of stray light and to mechanical or electrical shocks or interferences.

A schematic diagram of the detector block is shown in Fig. 2. It consists of the

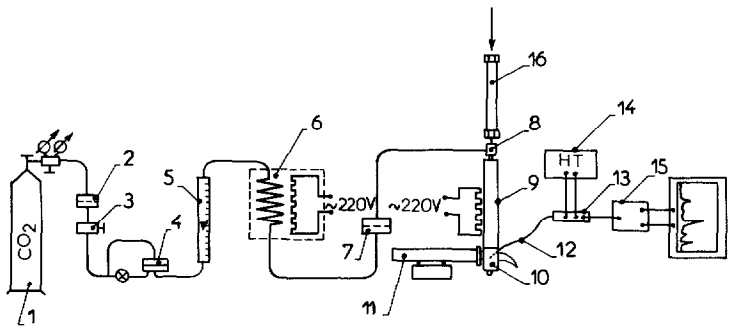

Fig. 1. Schematic diagram of the light-scattering detector with sample nebulization. 1 = CO_2 cylinder; 2 = Millipore filter; 3 = pressure controller; 4 = flow-rate controller; 5 = flow meter; 6 = oven; 7 = Millipore filter; 8 = nebulizer; 9 = heated block with drift tube; 10 = light-scattering cell; 11 = He–Ne laser; 12 = optical fibre; 13 = photomultiplier; 14 = high-voltage supply; 15 = electrometer; 16 = chromatographic column.

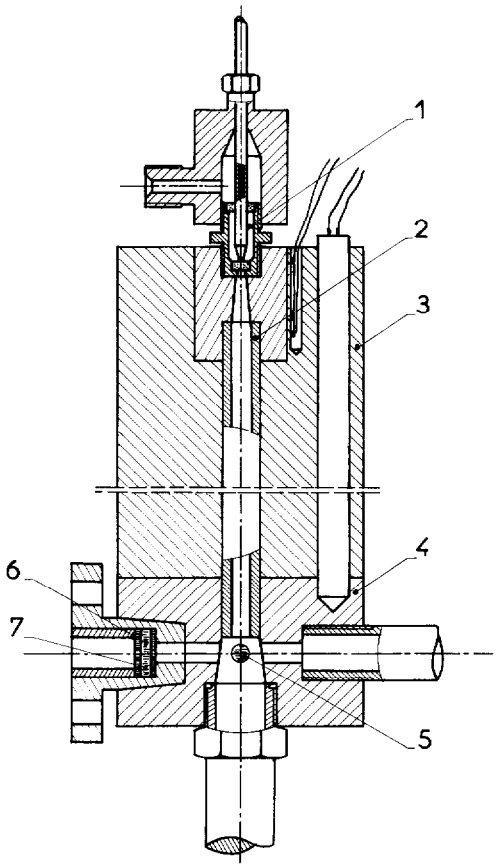

Fig. 2. Detector block. 1 = Nebulizer; 2 = drift tube; 3 = heated copper block; 4 = light scattering cell; 5 = glass rod; 6 = glass window; 7 = diaphragms.

nebulizer, a 30 cm × 2 mm I.D. drift tube (which can be coiled) enclosed in a heated copper block, and the light-scattering cell on the side of which a short piece of glass rod is placed perpendicular to the laser beam with the rod tip at the distance of 2 5 mm from the beam. The glass rod serves as a collector of scattered light.

The laser beam passes through a glass window located between two diaphragms and through the light-scattering cell, and impinges on to the "Reileigh horn" in which it is lost because of multiple reflections. This design generates a significant amount of stray light, however, resulting in increased background signal and noise. Work is in progress to improve the signal-to-noise ratio.

The nebulizer designs are shown in Fig. 3A and B. In the first design (Fig. 3A) the tip of a 0.25 mm I.D. capillary tube is pressed against a stainless-steel frit with 30-μm pores. The column eluate from this capillary is forced into the channels of the frit and nebulized by the driving gas which flows around the capillary tubing. This type of nebulizer is found to be efficient for moderate flow-rates of mobile phase of the order of 0.3–0.4 ml/min or larger. With smaller mobile phase flow-rates, considerable noise and spikes are observed. This phenomenon probably occurs as a result of diffusion of

driving gas bubbles into the channels of the frit, thus producing a non-uniform flow of liquid. This effect is even more pronounced with frits of smaller porosity, because higher pressures of driving gas are required to obtain a desired flow through the frit. This design is convenient for conventional 4 mm I.D. columns but would not be acceptable for 2 mm I.D. or narrower columns.

The nebulizer shown in Fig. 3B operates on a conventional principle. However, because of the required precision, it is more difficult to machine and assemble than the previous one. One end of a 0.25 mm I.D. capillary tube is connected to the outlet of the chromatographic column. The other end is soldered to a 0.15 mm I.D. short stainless-steel capillary tube positioned in the centre of a short 0.5 mm I.D. tube (3). Stainless-steel frits are used in order to localize exactly the capillary tube (2) in the centre of the tube (3). The performance of this "concentric" nebulizer is good at high flow-rates (0.3–0.5 ml/min), and also at low flow-rates down to 20–30 μl/min, and probably lower. With such a nebulizer, spikes still occur on the peak profiles, but to a much lesser extent than with the other design. Moreover, their height and frequency are independent of the mobile phase flow-rate and the spikes are easy to eliminate by software.

The response of the detector is studied by injecting small samples with a Rheodyne 7125 injection valve (Rheodyne, Berkeley, CA, U.S.A.) directly into the

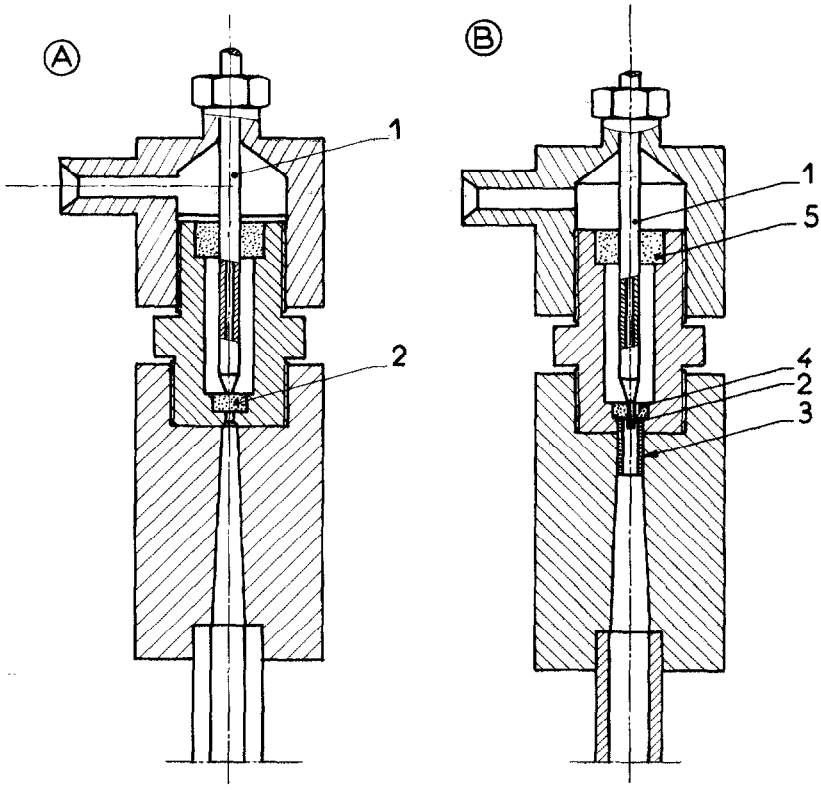

Fig. 3. Schematic diagrams of two nebulizers. (A) Nebulizer with stainless-steel fritted disc. 1 = Capillary tube, 0.25 mm I.D.; 2 = 30-μm stainless-steel frit. (B) Conventional concentric nebulizer. 1 = 0.25 mm I.D. tube; 2 = 0.15 mm I.D. stainless-steel tube; 3 = short 0.5 mm I.D. stainless-steel tube; 4 and 5 = stainless-steel fritted discs.

detector, without the use of a chromatographic column. The connection between the valve and the detector is designed to have the smallest possible dead volume. It is observed that with a 20-μl loop, the mobile phase volume necessary to sweep 20 μl of sample out of the system and restore a signal level close to the baseline (within 0.5 % of the recorder scale) is about 53 μl. The volumes injected are thus limited to 1 μl. The resulting profiles are unsymmetrical, requiring about 10 sec for the signal to return to the baseline, although more than 95 % of the sample is eluted during the first 3 sec at a flow-rate of 200 μl/min. The peak height is reproducible (R.S.D. 3 %), and is taken as a measure of the detector response.

RESULTS AND DISCUSSION

The flow-rate and temperature of the driving gas should be adjusted in such a way that the solvent is completely vaporized when the residual droplets reach the light-scattering cell. Typical operating conditions at flow-rates of 200–300 μl/min for mobile phases such as methanol, acetonitrile, acetone and chloroform are carbon dioxide flow-rate = 5 l (STP)/min and temperatures = 30 and 45–50°C for the oven and the drift tube, respectively. For water-containing solvents, the temperature should be increased to approximately 70°C for the oven and 80–85°C for the drift tube, with the same gas flow-rate. For smaller eluent flow-rates, lower temperatures are required.

Background current drift and noise

The dark current with the laser off at a photomultiplier polarization voltage of 630 V is $5 \cdot 10^{-12}$ A; the background current with the laser and driving gas on is $2 \cdot 10^{-10}$ A, and its noise is $1 \cdot 10^{-11}$ A. The background current, which is easily compensated in the amplifier, results mainly from stray light due to the dispersion of the laser beam by the glass window and back reflections in the home-made "Reileigh horn". The contribution of non-volatile solvent impurities to the background signal is negligible, as this signal does not change markedly when the solvent flow-rate is modified in the 50–300 μl/min range.

The only potential source of background signal drift is deposition of dust or aerosol on the inside of the glass window. Therefore, it is located outside the main stream of carrier gas, at some distance from the cell to prevent its contact with the particles. The drift is negligible. Background noise originates mainly from gas bubbles in the mobile phase and solid particles in the driving gas and the mobile phase. For this reason, tight Millipore filters are incorporated in both lines and solvents are degassed using an ultrasonic bath. Unlike what happens with other detectors, the noise on the peak profiles may be higher than the background noise. This phenomenon does not affect the detection level, but can reduce the precision in area measurements and thus the quantification. This noise is attributed to non-uniform nebulization and can indeed be reduced by improvements in the design and construction of the nebulizer. Spikes occuring occasionally during peak elution are due to a non-uniform flow of the eluent at the tip of the capillary tube (1 in Fig. 3A and B).

When the detector performances are studied by direct injection (without a chromatographic column), intense spikes are also created by droplets of insoluble or undissolved sample material.

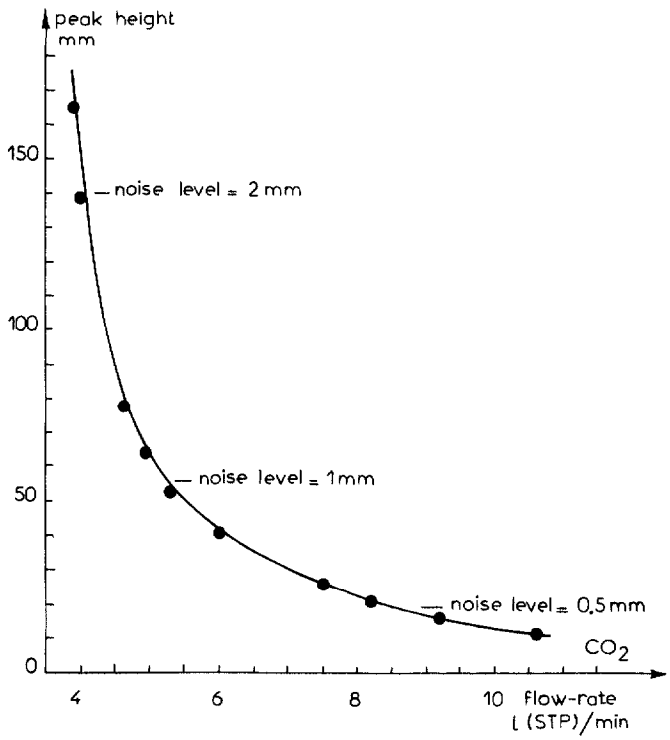

Fig. 4. Detector response as a function of the driving gas flow-rate. Mobile phase flow-rate, 200 μl/min; sample, glycerol (6 μg in 2 μl of methanol).

Influence of the driving gas flow-rate on the response

Both the signal and noise level decrease markedly with increasing flow-rate of the driving gas, as illustrated in Fig. 4. The signal-to-noise ratio is larger at relatively low flow-rates. Below 4 l (STP)/min, however, the noise increases rapidly, probably because of non-uniform nebulization. Thus the optimal flow-rate is between 4 and 5 l (STP)/min with this particular equipment. This value probably depends on the diameter of the drift tube but this effect was not further studied.

Influence of the temperature of the drift tube on the response

At constant temperature of the driving gas, the response of the detector for relatively volatile compounds depends on their vapour pressure. As expected, a plot of response *versus* temperature of the drift tube (Fig. 5) shows a steady decrease in response for methyl myristate (b.p. = 149.3°C at 1 mmHg) and methyl phthalate (b.p. = 283.8°C). The response for less volatile compounds, such as methyl oleate (b.p. = 218.5°C at 20 mmHg) and dioctyl phthalate (b.p. = 345°C at 20 mmHg) is relatively insensitive to temperature changes of the drift tube. There is a slight increase of the signal when the temperature of the drift tube is increased from ambient to about 45°C, for which we have no explanation at present.

The results are profoundly different for compounds that are solid at the drift tube temperature. The sensitivity may increase by nearly one order of magnitude

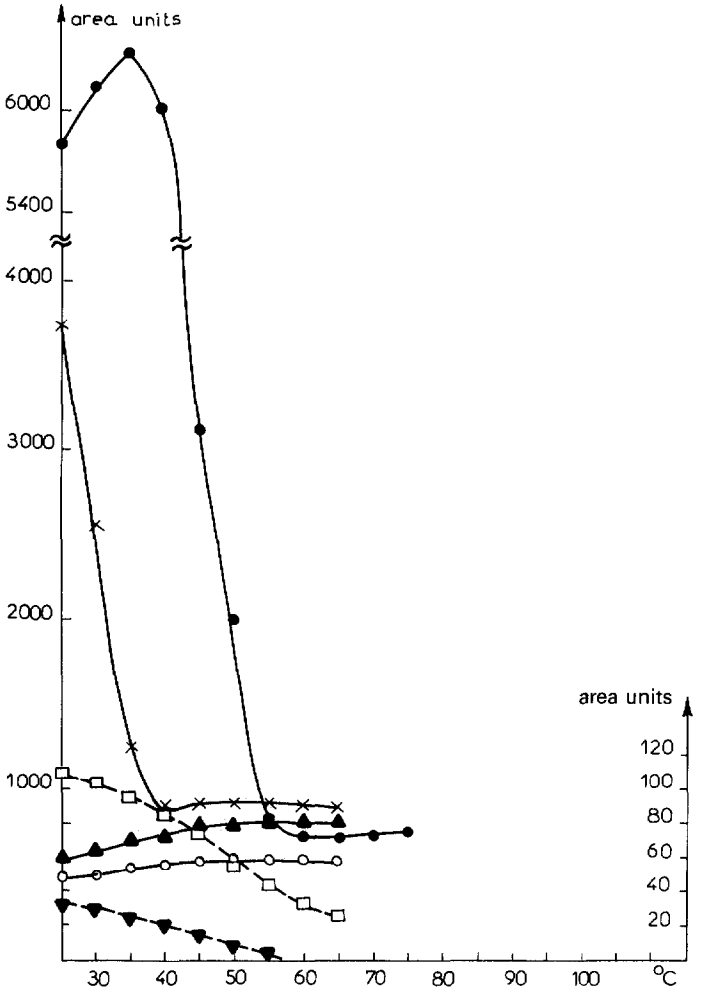

Fig. 5. Variation of detector response with temperature of the drift tube. Temperature of driving gas at nebulizer, 30°C; mobile phase, acetone; flow-rate, 200 μl/min. Solutes: ● = methyl arachidate (7.88 μg); × = methyl stearate (8.56 μg); ▲ = methyl oleate (7.74 μg); ○ = dioctyl phthalate (6.3 μg); ▼ = methyl myristate (2.85 μg); □ = dimethyl phthalate (7.35 μg). The signal scale for dimethyl phthalate and methyl myristate (right ordinate) is different from that for the other solutes (left ordinate).

when the drift tube temperature is decreased below their melting point. This phenomenon is due to a difference in the mechanism of light scattering when the particles are not spherical. Thus, light is more strongly scattered by snow flakes than by rain droplets. The response of the detector for methyl arachidate (m.p. = 54.5°C) and methyl stearate (m.p. = 39.1°C) are 9 and 4 times larger with drift tube temperatures of 25°C than of 60°C, respectively. A similar phenomenon was not observed with all solid compounds. For example, the response to sugars is much lower (but most sugars do not crystallize readily).

Relationship between response and sample size

As expected, the response is not linear. Fig. 6 shows a logarithmic plot of the

response *versus* sample size for compounds with different structures. Although a straight line is obtained over two orders of magnitude in sample size, the response is not linear as the slope is markedly different from unity. In fact, linear regression indicates that the average slope of the straight line log (signal) *versus* log (sample size) is 1.81 $\pm$ 2%. This shows that the mode of response is similar for all solutes included in Fig. 6.

This result is consistent with the mechanism of detection, as the intensity of the scattered light increases faster than the fourth power of the diameter of the droplets. When a peak is eluted, the number of droplets of solution in the nebulizer per unit time or volume of solvent remains constant, whereas the concentration of the solute in these droplets varies. Consequently, after solvent vaporization, the size of the droplets made of pure solute is proportional to the cube root of the solute concentration at the column outlet, as long as this concentration is large in comparison with that of the solvent impurities.

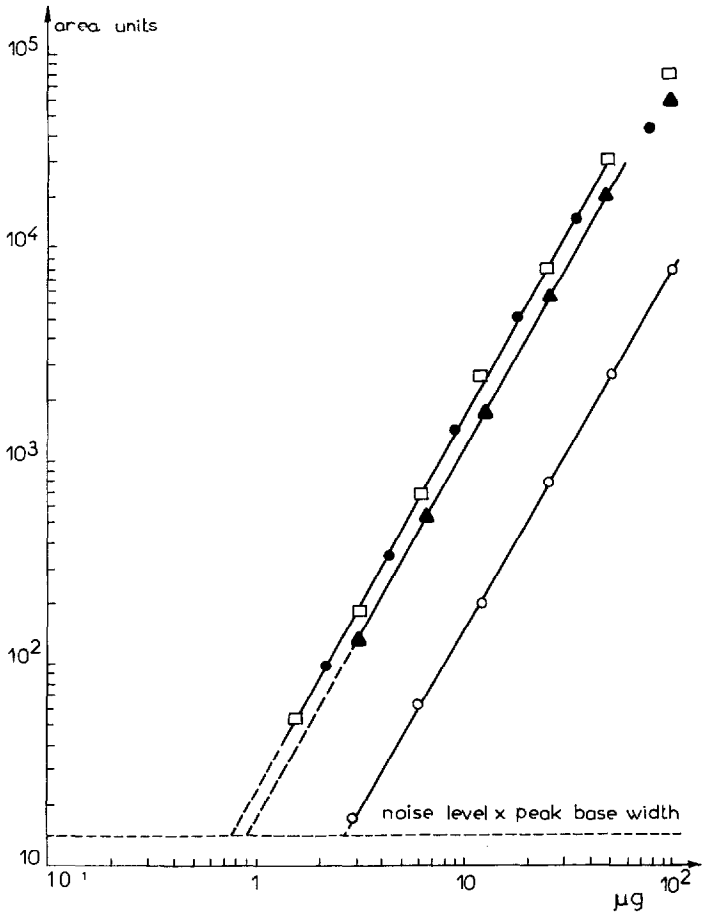

Fig. 6. Response of the detector *vs.* sample size for different compounds. Solvent, acetone, 200 µl/min (except for maltose, for which it was methanol, 200 µl/min); driving gas temperature, 30°C; drift tube temperature, 50°C. Solutes: □ = Dodecyl phthalate; ● = methyl linoleate; ▲ = glycerol; ○ = maltose.

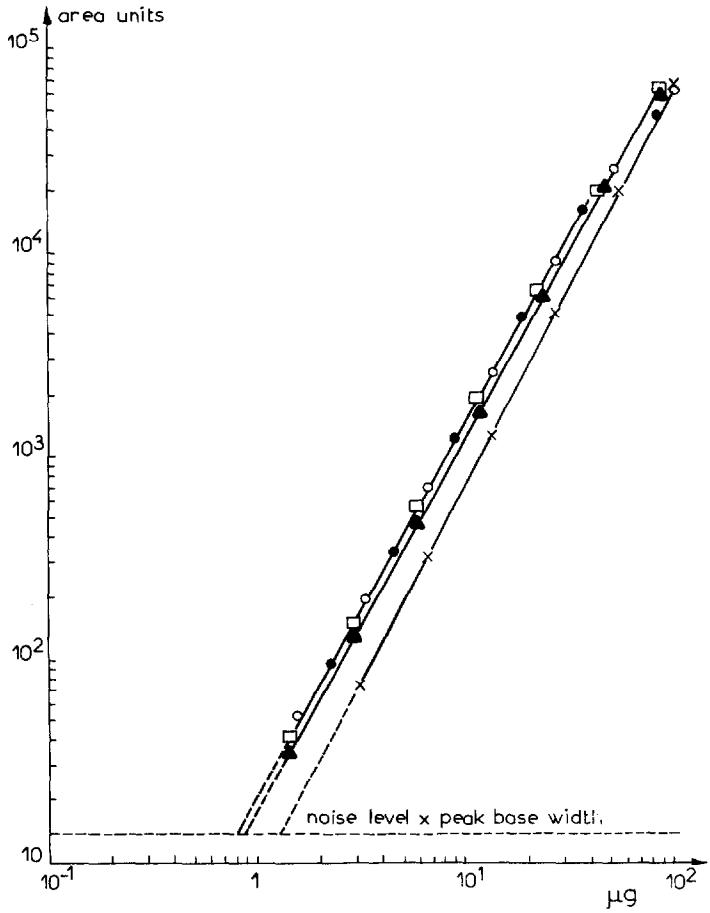

Fig. 7. Response of the detector *vs.* sample size for compounds with similar chemical structures. Solvent, acetone, 200 µl/min; drift tube temperature, 50°C. Solutes: ● = Methyl linolcate; □ = methyl olcate; ○ = methyl stearate; ▲ = methyl palmitate; × = methyl myristate.

Fig. 7 shows the changes in response with sample size for compounds of similar structures. These solutes are fatty acid methyl esters with either the same chain length but a different number of double bonds, or without double bonds but with different chain lengths (C_{14}, C_{16}, C_{18}). The response curves are almost indentical for all these compounds, except for methyl myristate. The smaller signal for this solute is due to partial vaporization in the drift tube, a phenomenon that has been already discussed. The slopes of the straight lines log (signal) *versus* log (sample size) obtained by linear regression are very similar for these solutes: 1.82 ± 1.6%.

The average slope for the seven compounds studied is 1.81 ± 1.7%. Finally, it must be pointed out that, for three solutes with identical carbon number (C_{18}), the values of the intercept of the response lines are similar (1.37, 1.37 and 1.40). The general trend seems to be a decrease in response with decreasing molecular weight (1.28 and 0.799 for C_{16} and C_{14}, respectively). This may be due to small losses by vaporization, or may reflect a more general phenomenon. More data are necessary to

discuss this point further. It is important to mention that the value of the response slope is not absolute, but depends on the design of the light scattering cell, and may be a function of the angle between the incident light beam and the axis of the collected scattered light beam. This point will be more thoroughly discussed in a forthcoming publication[23].

Detection limit

As the solvent is eliminated by vaporization, the detector responds only to the presence of solute particles crossing the laser beam, and to variations in their dimensions. Thus, the limit of detection, m_{DL}, is the mass of sample that generates a signal equal to a certain multiple of the background noise (2 in this work).

The concentration C_m of the solute at peak maximum and the sample mass flow-rate $\dot{m}$ can be calculated from the sample size m, the volume flow-rate F of mobile phase and the peak width at the base, ω, expressed in volume units (μl).

For a Gaussian profile, C_m is given by

$$C_m = \frac{m\sqrt{N}}{V_R\sqrt{2\pi}} = \frac{4m}{\omega\sqrt{2\pi}} \tag{1}$$

The sample mass flow-rate at peak maximum is

$$\dot{m} = C_m F = \frac{4mF}{\omega\sqrt{2\pi}} \tag{2}$$

The peak area A is related to the sample size and the response factr, ϱ, by

$$A = \varrho m^{1.81} \tag{3}$$

as shown above in Figs. 6 and 7. Accordingly, the peak height, H, is related to the mass flow-rate by

$$H = 1.81\ \varrho m^{0.81}\dot{m} = 2.89\ \varrho F m^{1.81}/\omega \tag{4}$$

The detection limit is that sample size which gives a peak height that is twice the noise:

$$m_{DL} = 0.69\left(\frac{\omega R}{\varrho F}\right)^{0.55} \tag{5}$$

where R is the noise and m_{DL} the detection limit. A 1.56-μg injection of glycerol at a flow-rate of 200 μl/min gives a signal of $15 \cdot 10^{-11}$ A. The band width is 20 μl and the noise is $1 \cdot 10^{-11}$ A. Thus, the response factor derived from eqn. 4 is 10.1 A sec $g^{-1.81}$ and the detection limit is 0.55 μg (eqn. 5). This corresponds to a concentration of 40 ppm in the mobile phase (eqn. 1) and a mass flow-rate of 140 ng/sec (eqn. 2). This is not very sensitive compared with the performances claimed for UVD or even conventional RID (1 ppm or less), but the great advantages of the detector discussed below compensate for this moderate sensitivity.

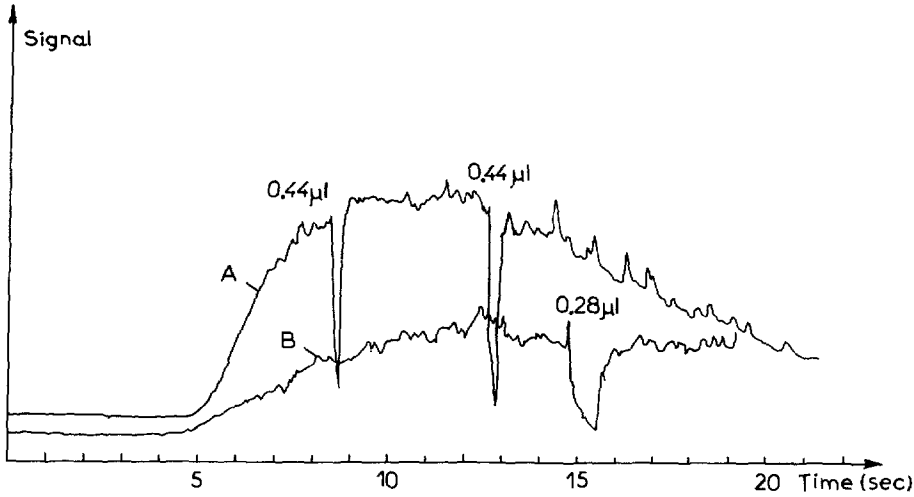

Fig. 8. Signals due to the injection of air bubbles within the sample. Mobile phase, methanol; flow-rate, (A) 100 µl/min and (B) 15.7 µl/min.

Contribution of the detector to band broadening

It is very difficult to measure this contribution as it is very small. The residence time of the sample in the detector can be calculated as the volume of the drift tube

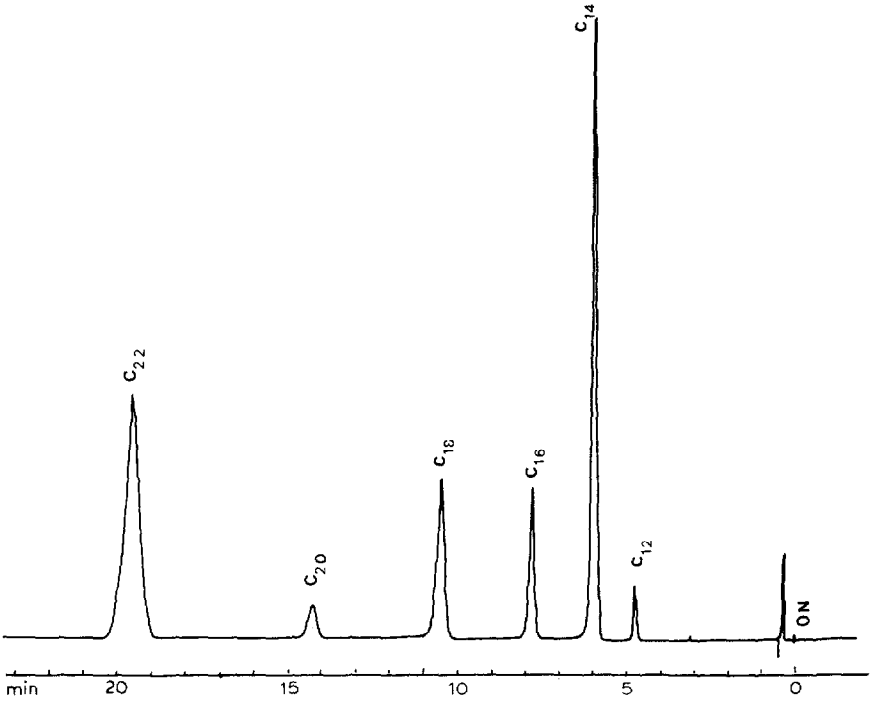

Fig. 9. Analysis of fatty acid methyl esters. Column, LiChrosorb RP-18 (5 µm), 200 × 2 mm I.D.; mobile phase, acetonitrile, 200 µl/min. Compounds: C_{12} = methyl laurate; C_{14} = methyl myristate; C_{16} = methyl palmitate; C_{18} = methyl stearate; C_{20} = methyl arachidate; C_{22} = methyl behenate.

(0.94 ml) divided by the driving gas flow-rate (4.5 l (STP)/min). It is approximately 12.5 msec and does not contribute much to band broadening.

The response time of the Keithley amplifier is 300 msec. The amplifier and the tube connecting the column to the nebulizer (3 cm × 0.25 mm I.D., 1.5 μl volume) are the weakest points. It would be possible to improve them markedly, if necessary.

The contribution of the detector to band broadening can be estimated from the signal obtained when an air bubble is injected within the sample. The sampling valve is directly connected to the detector without the column. As the residence time of the bubble in the system is very short, the solubility of air in the mobile phase can be ignored. Fig. 8 shows two traces obtained by injecting 20 μl of sample with 0.3- and 0.4-μl bubbles at mobile phase flow-rates of 100 and 15.7 μl/min, respectively (the bubble volumes are corrected for the pressure existing in the mobile phase flow line). As discussed above, the elution of such sample volume requires slightly more than 50 μl of solvent. The peaks corresponding to the bubbles are very sharp. In both instances, the signal returns to the baseline. This is consistent with a total contribution to band broadening of less than 0.15 μl, including the contributions of the connecting tubes and the nebulizer. This figure is much better than that which has been achieved so far with RID or with conventional UVD. Only by using on-column UV detection, the optical path being equal to the column diameter, was it possible to obtain mark-

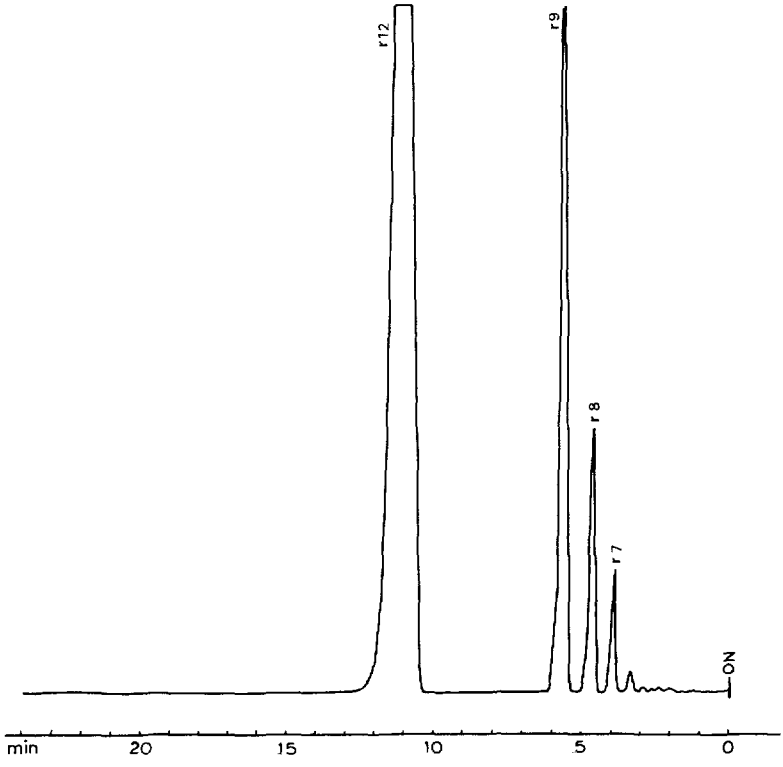

Fig. 10. Analysis of *n*-alkylbenzenes from *n*-hexyl- to *n*-dodecylbenzene. Conditions as in Fig. 9. The numbers on the peaks indicate the number of carbon atoms in the alkyl chains of the solute molecules.

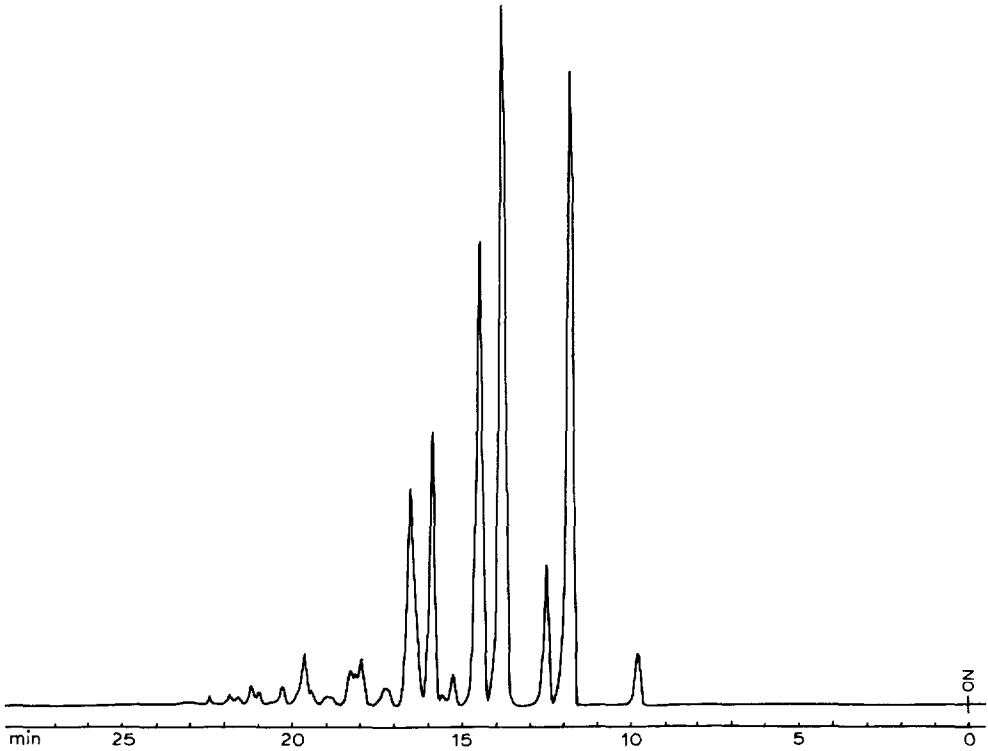

Fig. 11. Separation of the triglycerides of soyabean oil. Column, LiChrosorb RP-18 (5 μm), 200 × 2 mm I.D.; mobile phase, linear gradient from 33:67 acetone–acetonitrile to 99:1 acetone–acetonitrile in 25 min; flow-rate, 0.3 ml/min.

edly smaller values. Under these conditions, however, the sensitivity was dramatically decreased because of the short optical path length.

A more sophisticated method of measurement including the use of a straight capillary tube is being developed to evaluate accurately the detector cell volume and its contribution to band broadening.

Use of the detector under gradient elution conditions

The detector baseline is insensitive to changes of the composition of the mobile phase when mixtures of the following solvents are used: methanol, acetonitrile, acetone, chloroform, hexane and other light hydrocarbons. For water–methanol or water–acetonitrile mixtures, temperature programming of the drift tube must be used, otherwise the temperature is either too low for water-rich or too high for water-poor mixtures. Some examples are given in the applications discussed.

Examples of applications

Although this detector works best with non-volatile solutes, it can also be used to detect relatively volatile compounds if solvents with low boiling points are used. The experimental results suggest that quantitation is possible for solutes with boiling points above 280–300°C, such as dodecylbenzene, methyl palmitate and hexa-

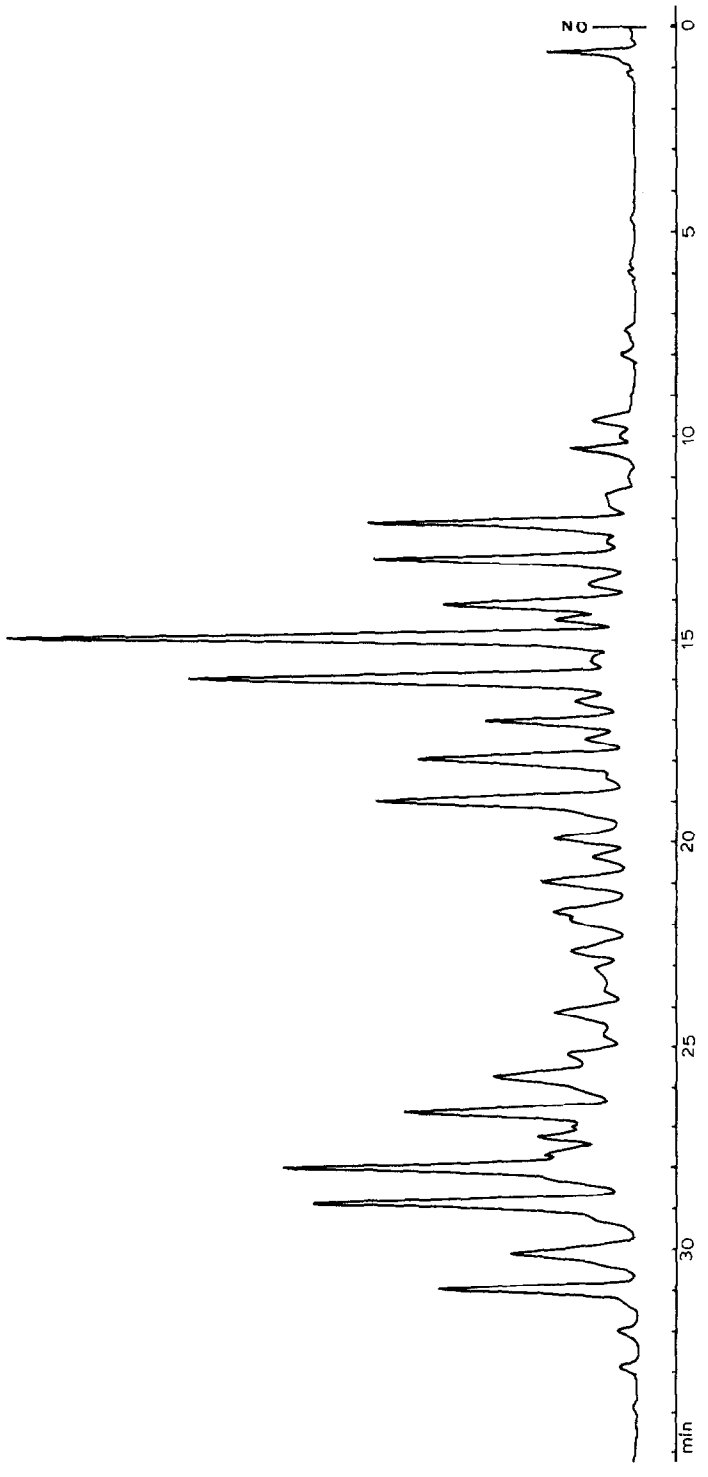

Fig. 12. Separation of butter fat triglycerides. Conditions as in Fig. 11.

decanol. Figs. 9–12 show some examples of separations. Note the absence of baseline drift in Figs. 11 and 12.

CONCLUSION

The performance of the light-scattering detector makes it especially attractive for the analysis of compounds that do not have a chromophore active above 200 nm and are present in complex mixtures that necessitate the use of gradient elution.

All non-volatile substances, mineral or organic, are easily detected, with a detection level which, in practice, compares favourably with that of the refractive index detector. The detector can be used with any solvent, solvent mixture or mobile phase gradient, as long as all eluent components are volatile. This eliminates a number of buffers. Finally, the contribution to band broadening is extremely small: only the recorder and amplifier used contribute significantly, and for fast analysis they should be replaced with faster systems. If the band broadening contribution is still too large at the flow-rate used, it could be reduced further by the use of a small scavenger flow without a significant decrease in sensitivity. This property gives the detector great potential for use in combination with narrow-bore packed columns, as long as the detection limit is adequate. Alternatively, the performances of the detector could be enhanced by a reduction of its dimensions, with a concurrent reduction in the flow-rate of the solvent used. At flow-rates below 100 μl/min, vaporization is very easily accomplished with minimum external heating.

The main drawbacks are the relatively low sensitivity, which could probably be improved by decreasing the amount of stray light, the non-linear response and the difficulties in determining very volatile compounds.

The geometry of the nebulizer is a critical factor of its efficiency. The flow-rate of the driving gas should be kept low, in order to increase the solute particle dimensions and thus the sensitivity of the detector. It is difficult at this stage to estimate the shape, average dimensions and size distribution of the particles that scatter light, and to clarify the response mechanism. Nevertheless, the factors that influence the particle size, *i.e.*, the sample size and the flow-rate of the driving gas, seem to have little effect on the slope of the response curve.

Work is continuing on the improvement of the nebulization technique, with the aim of reducing signal noise and detection limits, especially at low flow-rates.

ACKNOWLEDGEMENTS

One of us (A.S.) is grateful to the Scientific Exchange Agreement for a research fellowship. The technical assistance of Guy Preau was highly appreciated. We also acknowledge fruitful discussions with Michel Martin and Ante Krstulovic.

REFERENCES

1 R. P. W. Scott, *Liquid Chromatography Detectors*, Elsevier, Amsterdam, 1977.
2 H. Colin, A. Krstulovic and G. Guiochon, *Analusis*, 11 (1983) 155.
3 R. P. W. Scott and P. Kucera, *J. Chromatogr.*, 169 (1979) 51.
4 J. H. Knox and M. T. Gilbert, *J. Chromatogr.*, 186 (1979) 405.
5 G. Guiochon, *Anal. Chem.*, 53 (1981) 1318.

6 G. Guiochon, in P. Kucera (Editor), *Miniaturization of LC Equipment*, Elsevier, Amsterdam, 1983, in preparation.
7 P. Kucera and H. Umagat, *J. Chromatogr.*, 255 (1983) 563.
8 J. W. Jorgensen and E. J. Guthrie, *J. Chromatogr.*, 255 (1983) 335.
9 J. W. Jorgensen, S. L. Smiths and M. Novotný, *J. Chromatogr.*, 142 (1977) 233.
10 P. J. Arpino and G. Guiochon, *Anal. Chem.*, 51 (1979) 682A.
11 F. W. Willmot and R. J. Dolphin, *J. Chromatogr. Sci.*, 12 (1974) 695.
12 V. L. McGuffin and M. Novotný, *J. Chromatogr.*, 218 (1981) 179.
13 J. H. Charlesworth, *Anal. Chem.*, 50 (1978) 1414.
14 R. Macrae and J. Dick, *J. Chromatogr.*, 210 (1981) 138.
15 E. Haahti and T. Nikkari, *Acta Chem. Scand.*, 17 (1963) 2565.
16 A. T. James, J. R. Ravenhill and R. P. W. Scott, *Chem. Ind. (London)*, 18 (1964) 746.
17 E. Haahti, T. Nikkari and J. Korkkainen, in A. Goldup (Editor), *Gas Chromatography 1964*, Butterworths, London, 1964, p. 190.
18 A. T. James, J. R. Ravenhill and R. P. W. Scott, in A. Goldup (Editor), *Gas Chromatography 1964*, Butterworths, London, 1964, p. 197.
19 A. Stolyhwo, W. Erdahl and O. S. Privett, *J. Chromatogr. Sci.*, 11 (1973) 263.
20 J. G. Atwood, G. J. Schmidt and W. Slavin, *J. Chromatogr.*, 171 (1979) 109.
21 P. J. Arpino and G. Guiochon, *J. Chromatogr.*, 251 (1982) 153.
22 G. Mie, *Ann. Phys.*, 25 (1908) 377.
23 A. Stolyhwo, H. Colin and G. Guiochon, in prepartion.